npg

Photofrin binds to procaspase-3 and mediates photodynamic treatment-triggered methionine oxidation and inactivation of procaspase-3

Y-J Hsieh[1], K-Y Chien[1,2], S-Y Lin[3], S Sabu[1], R-M Hsu[3], L-M Chi[1,4], P-C Lyu[5] and J-S Yu*[,1,3]

Diverse death phenotypes of cancer cells can be induced by Photofrin-mediated photodynamic therapy (PDT), which has a decisive role in eliciting a tumor-specific immunity for long-term tumor control. However, the mechanism(s) underlying this diversity remain elusive. Caspase-3 is a critical factor in determining cell death phenotypes in many physiological settings. Here, we report that Photofrin-PDT can modify and inactivate procaspase-3 in cancer cells. In cells exposed to an external apoptotic trigger, high-dose Photofrin-PDT pretreatment blocked the proteolytic activation of procaspase-3 by its upstream caspase. We generated and purified recombinant procaspase-3-D_3A (a mutant without autolysis/autoactivation activity) to explore the underlying mechanism(s). Photofrin could bind directly to procaspase-3-D_3A, and Photofrin-PDT-triggered inactivation and modification of procaspase-3-D_3A was seen *in vitro*. Mass spectrometry-based quantitative analysis for post-translational modifications using both $^{16}O/^{18}O$- and $^{14}N/^{15}N$-labeling strategies revealed that Photofrin-PDT triggered a significant oxidation of procaspase-3-D_3A (mainly on Met-27, -39 and -44) in a Photofrin dose-dependent manner, whereas the active site Cys-163 remained largely unmodified. Site-directed mutagenesis experiments further showed that Met-44 has an important role in procaspase-3 activation. Collectively, our results reveal that Met oxidation is a novel mechanism for the Photofrin-PDT-mediated inactivation of procaspase-3, potentially explaining at least some of the complicated cell death phenotypes triggered by PDT.
Cell Death and Disease (2012) 3, e347; doi:10.1038/cddis.2012.85; published online 12 July 2012
Subject Category: Immunity

Photodynamic therapy (PDT) has a direct effect on cancer cells, triggering cell death by autophagy, apoptosis and/or necrosis.[1–3] It was initially believed that PDT killed cells via necrosis, but in 1991, Oleinick and colleagues[4] demonstrated that PDT could trigger apoptosis of mouse lymphoma cells. Numerous subsequent studies (including ours) documented that different cell death phenotypes can be induced by PDT, depending on the cell type, the photosensitizer and its subcellular location, the overall dose and the incubation protocol.[5–9] Several reports have shown that Photofrin-PDT can have complicated effects on tumor cells, where either apoptosis or necrosis has been observed.[5] However, although many reports have documented the complicated cell death phenotypes induced by PDT, less attention has been paid to the effect of PDT on the modification and regulation of caspase-3 activity, which is a critical factor in determining cell death phenotypes.

Caspase-3, an important executioner in apoptosis, exists in cells as an inactive zymogen and can be activated by proteolysis through either the intrinsic mitochondria-mediated pathway or the extrinsic death-receptor-mediated pathway.[10]

Owing to its critical role in apoptosis, numerous reports have investigated the regulation of caspase-3 activity by different post-translational modifications, such as nitrosylation, glutathionylation and phosphorylation, all of which inhibited caspase-3 activity.[11–13] However, it is currently unknown whether caspase-3 could be affected and modified by other reactive oxygen species (ROS), such as the singlet oxygen elicited by clinically approved PDT.

Some studies have shown that caspase-3 was activated by PDT, whereas others found that PDT-induced necrosis occurred without caspase-3 activation.[3,14,15] In this study, we detected significant inhibition of caspase-3 activation exposed to higher (but not lower) doses of Photofrin-PDT, and which could dose-dependently induce covalent modification of procaspase-3 in human cells. We generated and purified recombinant procaspase-3 to confirm the direct inactivation and modification of procaspase-3 by high-dose Photofrin-PDT *in vitro*. In addition, we used $^{16}O/^{18}O$- and $^{14}N/^{15}N$-labeling methods coupled with liquid chromatography-electrospray tandem mass spectrometry (LC-MS/MS) to quantitatively analyze procaspase-3, and found that methionine oxidation

was the major modification mode caused by Photofrin-PDT. Finally, we observed that Met-44, one of the major modification sites, has an important role in the activation of procaspase-3.

Results

Photofrin-PDT elicits a bell-shape, dose-dependent activation of caspase-3 in human cancer cell lines. Caspase activation has critical roles in determining the cell death phenotype in PDT treatment, but conflicting reports existed regarding the effects of PDT on the cell death phenotype.[14–16] Here, we performed caspase-3 activity assays in cells treated with different doses of Photofrin followed by PDT. We found that Photofrin-PDT elicited a bell-shape, dose-dependent activation of caspase-3 in both A431 and Jurkat T cells (Figures 1a and d). Caspase-3 activity increased following PDT of cells that received Photofrin doses of 7–14 μg/ml, but decreased drastically when the Photofrin dose was ≥28 μg/ml. We also found that staurosporine, a well-known apoptotic trigger for many cell types,[17] could further activate caspase-3 in cells pretreated with Photofrin-PDT. However, the extent of further activation by staurosporine was significantly lower in cells receiving PDT at higher doses (28–112 μg/ml) of Photofrin (Figures 1a and d, compare the gray and white bars). The death phenotypes of both cells treated with different doses of Photofrin-PDT were evaluated by annexin V and propidium iodide staining. The results showed that although apoptosis could be slightly and moderately triggered in A431 and Jurkat T cells, respectively, by lower doses (7–14 μg/ml) of Photofrin-PDT, necrotic-like cell death represented the major death phenotype in both cells that received higher doses (28–112 μg/ml) of Photofrin-PDT (Figures 1b and e). We additionally examined the effect of Photofrin-PDT on the TRAIL or FasL-mediated apoptotic cell death in Jurkat T cells and found that PDT with 28 μg/ml of Photofrin could significantly attenuate the anti-Fas antibody- and TRAIL-mediated caspase-3 activation (Supplementary Figure 1). This finding indicates that high-dose Photofrin-PDT can impair the caspase-3 activation elicited by an apoptotic trigger in both A431 and Jurkat T cells.

To explore further, extracts of A431 cells treated with or without Photofrin-PDT were immunoblotted with an anti-caspase-3 antibody. To our surprise, in addition to the expected 32-kDa procaspase-3 protein, we also observed the Photofrin dose-dependent appearance of an unusual high molecular weight (HMW) species (>80 kDa) with immunoreactivity to the anti-caspase-3 antibody (Figure 1c), which could also be observed in Photofrin-PDT-treated Jurkat T cells (Figure 1f). The specificity of anti-caspase-3 antibody was further confirmed using extracts of MCF-7 cells lacking caspase-3 expression[18] (Supplementary Figure 2). Consistent with our above findings, PDT with low doses (14 and 28 μg/ml) but not high doses (56–112 μg/ml) of Photofrin could activate caspase-3 in Jurkat T cells as evidenced by immunoblotting (Figure 1f, lower panel). Regarding A431 cells, the p17 subunit could not be detected clearly under the same assay condition (data not shown). Moreover, we found the selectivity of Photofrin-PDT to modify caspase-3 but not

caspase-8 and -9 (Supplementary Figure 3). Collectively, these results show that Photofrin-PDT has a dose-dependent biphasic effect on caspase-3 activation, and also suggest that Photofrin-PDT may cause covalent modification of caspase-3 in cells.

High-dose Photofrin-PDT inhibits caspase-8-mediated cleavage/activation of caspase-3 in A431 cell lysates. On the basis of the above observations, we hypothesize that after PDT, procaspase-3 may lose its capability to be processed by upstream caspase-8,[10] or its processed product(s) of caspase-3 might lose their enzyme activity via covalent modifications elicited by Photofrin-PDT. As expected, the endogenous procaspase-3 in the control lysates was efficiently processed by exogenous caspase-8 (Figure 1g, compare lanes 3, 5 and 7). However, the active subunits were barely detected in lysates pretreated with Photofrin-PDT (Figure 1g, lanes 4, 6 and 8). These results collectively suggest that Photofrin-PDT may modify procaspase-3 to a form that is not properly processed by caspase-8. The major effect of PDT is to generate ROS, and we found that in the presence of sodium azide (a potent ROS scavenger), Photofrin-PDT could no longer inhibit the caspase-8-mediated proteolytic activation of procaspase-3 (Figure 1h). This observation further indicated that Photofrin-PDT-generated ROS are required for caspase-3 modification(s).

Photofrin-PDT directly elicits the chemical modification and enzymatic inhibition of procaspase-3. To further investigate the mechanism responsible for this effect, we generated and purified recombinant procaspase-3 for further studies. Consistent with previous reports,[19] the recombinant procaspase-3 produced in *Escherichia coli* degraded and quickly autoactivated during purification, producing processed/activated caspase-3 that was not suitable for the present study. We thus generated procaspase-3 mutant (procaspase-3-D_3A),[20] in which three Asp residues, Asp-9, -28 and -175, were substituted to Ala to prevent autocleavage/activation during purification (Figure 2a). When purified procaspase-3-D_3A was treated by Photofrin-PDT, the formation of HMW species resembling those detected in cells was observed (Figure 2b, compare lanes 1 and 2), indicating that cross-linking occurred among the procaspase-3-D_3A monomers. In addition to the formation of HMW species, PDT also caused a slight molecular weight shift of the 32-kDa procaspase-3-D_3A, resulting in the formation of a clear doublet on the SDS gel (Figure 2b, lane 4); this suggests that PDT can cause complex modifications of procaspase-3-D_3A. We also found that Photofrin-PDT suppressed the caspase-3 activity assayed by Ac-DEVD-pNA in a Photofrin dose-dependent manner (Figure 2c). Similar results were observed when we monitored polyADP-ribose polymerase (PARP) as an endogenous substrate (Figure 2d, compare lanes 1–3). Moreover, sodium azide pretreatment significantly attenuated the Photofrin-PDT-mediated suppression of caspase-3 activity (Figure 2d), again indicating that the ROS have a critical role in this effect.

We found that after PDT with 28 μg/ml Photofrin, the protein ratio of the HMW species to procaspase-3-D_3A (32 kDa)
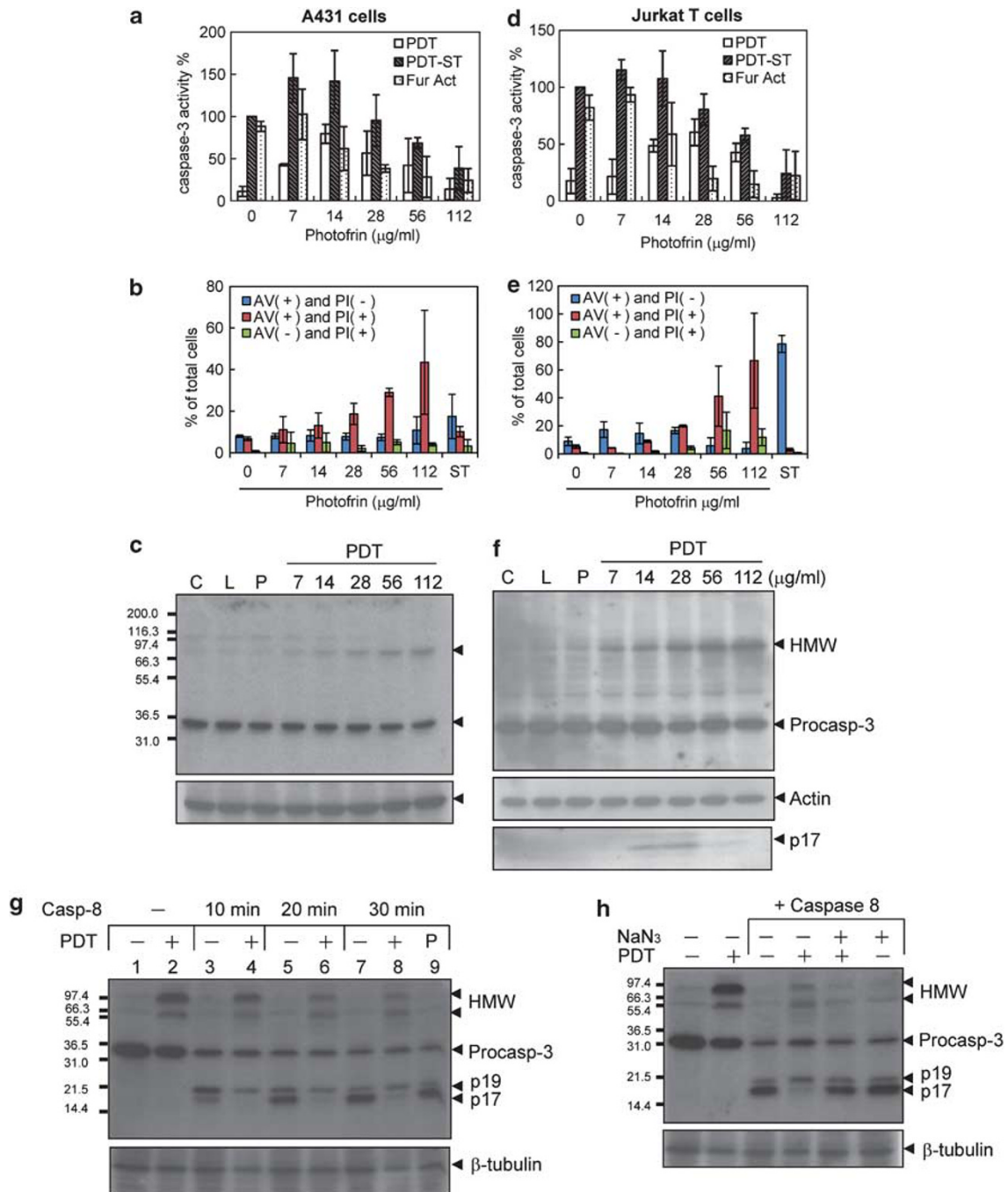
Figure 1 Effects of Photofrin-PDT on the activation and modification of procaspase-3. (**a**) A431 cells were treated with different doses of Photofrin-PDT, and then immediately treated with staurosporine (ST, 1 μM) for another 6 h. Cell lysates (100 μg) were analyzed for caspase-3 activity using Ac-DEVD-pNA as a substrate. PDT, cells were treated with PDT alone; PDT-ST, cells were treated with PDT and ST; Fur Act, the activity difference between PDT-ST and PDT, which denotes further activation by ST. (**b**) A431 cells were treated with different doses of Photofrin-PDT, and after PDT, the cells were incubated for another 6 h. The cells were then harvested for annexin V (AV)/propidium iodide (PI) staining and flow cytometry analysis. The percentage of positively ($+$) and negatively ($-$) stained cells for AV/PI in each condition were indicated. Cells treated with staurosporine (ST, 1 μM) for 6 h were used as control. (**c**) A431 cells were treated with or without different doses of Photofrin-PDT, and cell extracts (20 μg) were subjected to 10% SDS-PAGE followed by immunoblot analysis with an anti-caspase-3 antibody. C, untreated; L, laser alone for a total of 10 J with a fluence rate of 15 mW; P, 28 μg/ml Photofrin alone. Actin (lower panel) was detected as the internal control. (**d–f**) Jurkat T cells were treated and analyzed as described in (**a–c**), respectively. The resulting cell lysates (20 μg in the upper panel and 100 μg in the lower panel) were subjected to immunoblot analysis with an anti-caspase-3 antibody. (**g**) A431 cell extracts (100 μg) were left untreated ($-$), treated with 28 μg/ml of Photofrin followed by PDT ($+$), or treated with 28 μg/ml of Photofrin alone (P). Recombinant active caspase-8 (0.3 U) was then added, and the extracts were incubated at 37°C for 10–30 min in the dark. The reaction products were resolved by SDS-PAGE and analyzed by immunoblotting with an anti-caspase-3 antibody. (**h**) A431 cell lysates were pretreated without ($-$) or with ($+$) 5 mM NaN$_3$, followed by treatment with or without PDT using 28 μg/ml of Photofrin. The cell lysates (100 μg) were then prepared and processed by caspase-8 for 30 min as described in (**g**)

a
```
MENTENSVAS KSIKNLEPKI IHGSESMASG ISLDNSYKMD YPEMGLCIII
NNKNFHKSTG MTSRSGTDVD AANLRETFRN LKYEVRNKND LTREEIVELM
RDVSKEDHSK RSSFVCVLLS HGEEGIIFGT NGPVDLKKIT NFFRGDRCRS
LTGKPKLFII QACRGTELDC GIETASGVDD DMACHKIPVE ADFLYAYSTA
PGYYSWRNSK DGSWFIQSLC AMLKQYADKL EFMHILTRVN RKVATEFESF
SFDATFHAKK QIPCIVSMLT KELYFYHLEH HHHHH
```
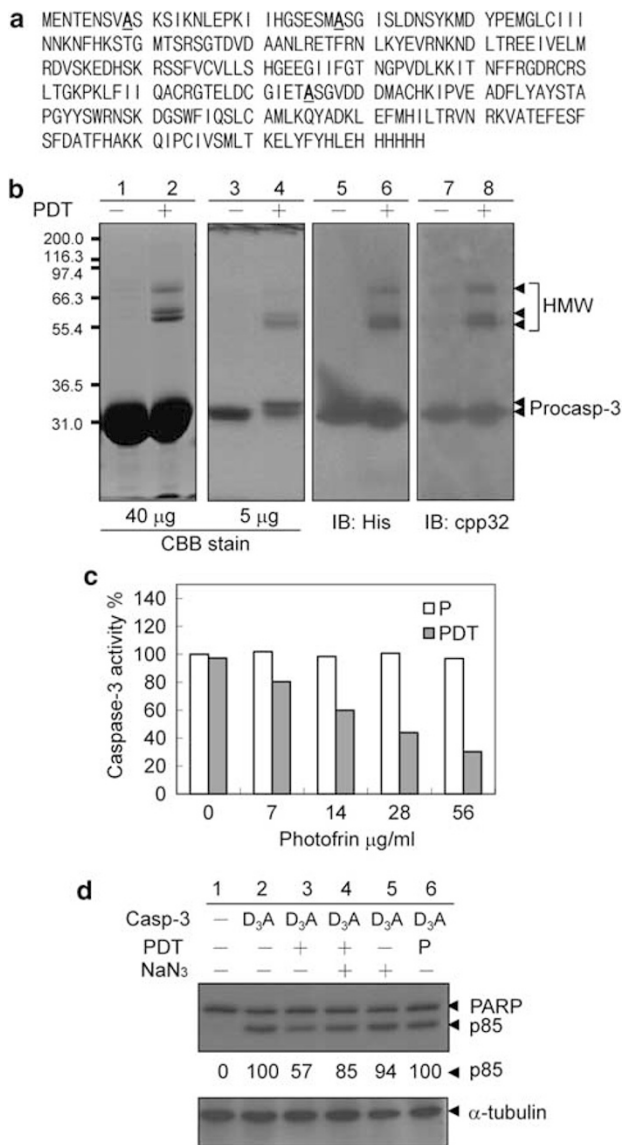
Figure 2 Photofrin-PDT causes inactivation and modification of recombinant procaspase-3-D$_3$A. (**a**) The amino-acid sequence of the recombinant human procaspase-3-D$_3$A protein. The protein was Ala-mutated at Asp-9, Asp-28 and Asp-175 (underlined) and COOH-terminal tagged with six His residues. (**b**) Recombinant procaspase-3-D$_3$A was left untreated (–) or treated with PDT (+) using 28 μg/ml of Photofrin, resolved by 10% SDS-PAGE, and then subjected to Coomassie brilliant blue staining (CBB) and immunoblotting with anti-His or anti-caspase-3 antibodies. (**c**) Recombinant procaspase-3-D$_3$A (10 μg) was incubated with different doses of Photofrin in the dark for 10 min, left in the dark (P) or irradiated with laser (PDT), and then examined by the colorimetric caspase-3 activity assay as described. The experiments were repeated three times with reproducible results. (**d**) Recombinant procaspase-3-D$_3$A (10 μg) was left untreated (–) or treated (+) with Photofrin-PDT in the absence (–) or presence (+) of 5 mM NaN$_3$. After treatment, A431 cell lysates (100 μg) were mixed individually with the variously treated recombinant procaspase-3-D$_3$A proteins and incubated at 37°C for 1 h in the dark. The reaction products were resolved by 10% SDS-PAGE and subjected to immunoblotting with an anti-PARP antibody. Actin (lower panel) was detected as an internal control. The positions of PARP and its p85 cleavage fragment are denoted by arrows, and the p85 signal was quantified by densitometry

was ~ 1/10 to 1/5, but the activity was only 40% of the control level (Figures 2b and c). This finding suggests that covalent modification(s) by small chemical group(s), which we believe cause the slight molecular weight shift of the 32-kDa procaspase-3-D$_3$A, could have a major role in the Photofrin-PDT-mediated suppression of caspase-3 activity.

Direct interaction between procaspase-3-D$_3$A and Photofrin. Photofrin-PDT can trigger the immediate production of ROS,[21] which are directly involved in the modification and inactivation of procaspase-3 (Figure 2d). As ROS are highly reactive and have a short half-life, PDT-generated ROS would be likely to affect only components in the vicinity of their production (i.e., adjacent to the photosensitizer). This prompted us to test whether Photofrin can directly bind to procaspase-3-D$_3$A by gel filtration. As shown in Figure 3a, procaspase-3-D$_3$A yielded a minor peak (fraction 8) and a major peak (fraction 13) for optical density at 280 nm but barely emitted fluorescence at 630 nm, whereas Photofrin had a fluorescence peak (fraction 14) but showed very low absorption at 280 nm. However, when a mixture of Photofrin and procaspase-3-D$_3$A was resolved, two prominent fluorescence peaks emerged at fractions 8 and 11 (Figure 3a, lower panel). Subsequent dot-blot analysis of these fractions (Figure 3b) showed that: (i) Photofrin alone did not bind significantly to the PVDF membrane; (ii) procaspase-3-D$_3$A alone was distributed mainly in fractions 10–14 with a minor part in fraction 8, and did not emit a fluorescence signal; and (iii) when the mixture of Photofrin and procaspase-3-D$_3$A was resolved, the signals for procaspase-3-D$_3$A and Photofrin co-existed in fractions 8–15. These observations suggest that Photofrin can bind to and co-elute with procaspase-3-D$_3$A during gel filtration. To explore further, other proteins (e.g., bovine serum albumin, ovalbumin and casein) were spotted in parallel as controls. We found that only the spots containing procaspase-3-D$_3$A showed clear Photofrin signals above the background level (Figure 3c). These results collectively indicate that Photofrin can selectively and directly interact with procaspase-3-D$_3$A.

Analysis of Photofrin-PDT-elicited modification of procaspase-3-D$_3$A using ^{16}O/^{18}O- and ^{14}N/^{15}N-labeling-based quantitative proteomics strategies. To examine possible modifications of procaspase-3-D$_3$A and whether Photofrin is covalently linked to procaspase-3-D$_3$A, we first used Fourier transform ion cyclotron resonance MS to measure the molecular mass of procaspase-3-D$_3$A before and after Photofrin-PDT. The mass differences were found to be + 16 Da and + 32 Da (Supplementary Figure 4), strongly suggesting that Photofrin-PDT can elicit oxidation of procaspase-3-D$_3$A by adding one or two oxygen atoms to the protein. This observation seems to preclude the possibility that porphyrin monomer(s) (580 Da for each monomer) were covalently incorporated into procaspase-3-D$_3$A during Photofrin-PDT. It is well known that PDT can induce oxidation of some proteins such as GRP-78 and Bcl-2.[22,23] Our results also suggested that oxidation may represent the major type of procaspase-3-D$_3$A modification elicited by Photofrin-PDT. We next used ^{16}O/^{18}O- and ^{14}N/^{15}N-labeling-based quantitative proteomics strategies in conjunction with the accurate
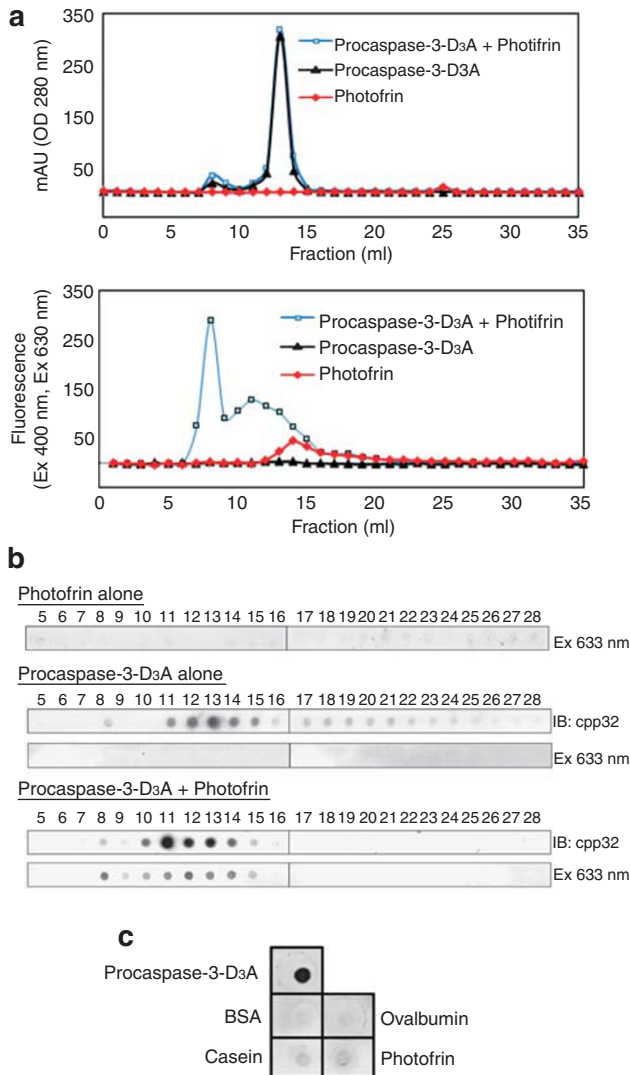
Figure 3 Gel filtration analysis of the interaction between Photofrin and recombinant procaspase-3-D$_3$A. Recombinant procaspase-3-D$_3$A alone (1 mg), Photofrin alone (18.13 μg) or recombinant procaspase-3-D$_3$A (1 mg) plus Photofrin (18.13 μg) (molar ratio 1 : 1) were applied to Superose 12 columns for gel filtration analysis, as described. (**a**) Each fraction was subjected to optical density measurement (280 nm) for procaspase-3-D$_3$A proteins and fluorescence measurement (excitation 400 nm and emission 630 nm) for Photofrin. (**b**) Fractions were also directly spotted onto a PVDF membrane, and procaspase-3-D$_3$A and Photofrin signals were detected by immunoblotting and fluorescence scanning (Typhoon 9400), respectively. (**c**) Procaspase-3-D$_3$A, bovine serum albumin (BSA), ovalbumin, casein (10 μg of each protein) or Photofrin (5 μg) were spotted onto a PVDF membrane. The membrane was incubated with Photofrin-containing solution (100 μg in 10 ml distilled water) at room temperature in the dark for 3 h, washed thrice for 10 min with distilled water and thrice for 10 min with TTBS buffer (20 mM Tris-HCl, pH 7.4, 0.5 M NaCl, and 0.05% Tween 20). The washed membrane was air-dried and then scanned by a Typhoon 9400 fluorescence scanner

mass and time tag approach to systemically identify and quantify the Photofrin-PDT-modified amino-acid residues of procaspase-3-D$_3$A (Supplementary Figure 5–8).[24] We obtained a list of possible modifications from the LC-MS/MS data and the relative abundance ratios of all identified pairs of ^{16}O/^{18}O-labeled peptides from the LC-MS data

(Supplementary Table 1). Most of the detected peptide pairs had ratios of 0.79–1.5, and Table 1 lists 13 peptide pairs with relative abundance ratios $\geq$ 1.5. Notably, 12 out of the 13 had at least one oxidized methionine (oxiMet) residue. In fact, 8 of the 10 Met residues in procaspase-3-D$_3$A (Met-27, -39, -44, -100, -182, -222, -233 and -268) showed increased oxidation ($\geq$ 1.5-fold) after PDT. We further used a more accurate ^{15}N-labeling-based quantitative proteomics strategy (labeling at protein level) to analyze the PDT-elicited Met oxidation of procaspase-3-D$_3$A at different Photofrin doses (Supplementary Figure 8). The quantitation results for all of the detected peptides are shown in Supplementary Table 2. We first analyzed the amounts of unmodified precursor peptides remaining after PDT with four different Photofrin doses. PDT with higher doses of Photofrin (28 and 56 μg/ml) caused significant decreases in the precursor peptides; the N-terminal region (a.a. 1–53) and internal region (a.a. 165–186) showed the most drastic reductions (30–40%) (Figure 4a). We then calculated the oxidized peptide yields after PDT; 7 out of the 10 Met residues (Met-27, -39, -44, -100, -182, -233 and -268) of procaspase-3-D$_3$A showed Photofrin dose-dependent increases of oxidized peptide yields after PDT (Table 2). Figure 4b shows the oxidized peptide yields of all identified peptides following PDT with different Photofrin doses. It is interesting to note that two peptides, [20]IIHGSESMASGISLDNSY[38]K (containing oxiMet-27) and [39]MDYPEMGLCIIINN[53]K (containing oxiMet-39 and oxiMet-44) showed drastic increases in the oxidized peptide yield after PDT; their oxidized yields could reach 40.81 and 75.06% after 56 μg/ml Photofrin-PDT, respectively (Table 2). This suggests that Met-27, -39 and -44 may represent the most vulnerable residues for PDT. Moreover, the oxidized forms of [39]MDYPEMGLCIIINN[53]K could together account for as much as 75.06% of the total detected forms of this peptide, and this value is similar to the extent of caspase-3 activity decrease seen after PDT with 56 μg/ml of Photofrin (Figure 2c). Notably, no oxidized peptide pairs for [157]LFII-QAC[164]R were detected in both ^{16}O/^{18}O and ^{14}N/^{15}N-labeling analysis, suggesting that the catalytic site Cys-163 might not be modified by PDT. Taken together, these results suggest that PDT-induced methionine oxidation might represent the major event leading to the inhibition of procaspase-3-D$_3$A.

Substitution of Met-44 by Leu significantly attenuates the proteolytic maturation of caspase-3. We next questioned whether these Met residues have critical roles in caspase-3 activity regulation. However, there is no available method for creating targeted and site-specific Met oxidations in a protein. Thus, we studied the role of the three Met residues by substituting each of them with leucine, which has a high stereo-structural similarity to methionine. We generated M27L, M39L and M44L mutants of procaspase-3-D$_3$A, respectively, and assayed the purified mutants for caspase-3 activity before and after PDT. Before PDT, the D$_3$A-M27L and D$_3$A-M39L mutants displayed activities comparable to that of procaspase-3-D$_3$A. In contrast, the activity of the D$_3$A-M44L mutant was drastically lower ($\sim$ 50%) than that of procaspase-3-D$_3$A (Figure 5a), indicating that Met-44 may have an important role in regulating caspase-3 activity

Table 1 List of 13 tryptic peptides of procaspase-3-D$_3$A that showed >1.5-fold increases after Photofrin-PDT, as assessed by ^{18}O labeling

Start	Stop	Peptide sequence	Modifications	Charge	Observed MS	Theoretical MS	Ion score	Identity score	Expect value	PDT/Ctrl ratio (mean ± SD)
20	38	IIHGSESMASGI SLDNSYK	Oxidation M (+15.99)	2.3	675.65	2023.95	131.0	56.3	1.60E-09	5.07 ± 1.85
39	53	MDYPEMGLCIIINNK	Oxidation (+15.99) M39, Carbamidomethyl (+57.02)	2	913.93	1825.84	78.6	55.3	2.40E-04	1.64 ± 1.08
39	53	MDYPEMGLCIIINNK	Oxidation (+15.99) M44, Carbamidomethyl (+57.02)	2	913.93	1825.84	80.6	55.3	1.50E-04	2.34 ± 0.91
94	101	EEIVELMR	Oxidation M (+15.99)	1.2	517.77	1033.51	51.2	33.8	NA	2.09 ± 0.60
165	186	GTELDCGIETASGV DDDMACHK	Carbamidomethyl (+57.02), Oxidation M (+15.99), Carbamidomethyl (+57.02)	2.3	1198.98	2395.96	122.0	45.6	1.10E-09	1.50 ± 0.37
211	224	DGSWFIQSLCAMLK	Carbamidomethyl (+57.02), Oxidation M (+15.99)	2	836.40	1670.78	61.6	56.3	1.50E-02	4.44 ± 1.69
225	238	QYADKLEFMHILTR	Gln->pyro-Glu (N-term Q) (−17.03), Oxidation M (+15.99)	2	882.44	1762.87	90.0	37.0	NA	1.96 ± 1.00
225	238	QYADKLEFMHILTR	Oxidation M (+15.99)	2	890.96	1779.90	62.0	57.0	1.60E-02	2.28 ± 0.73
230	238	LEFMHILTR	Oxidation M (+15.99)	2	588.31	1174.62	69.3	57.9	3.60E-03	1.74 ± 0.94
242	259	KVATEFESFSFDATFHAK		2.3	688.01	2060.98	145.0	56.9	8.50E-11	1.51 ± 0.66
260	271	KQIPCIVSMLTK	Carbamidomethyl (+57.02), Oxidation M (+15.99)	2	717.38	1432.78	73.9	57.5	1.10E-03	1.71 ± 0.42
261	271	QIPCIVSMLTK	Carbamidomethyl (+57.02), Oxidation M (+15.99)	2	653.34	1304.68	47.2	34.8	NA	1.62 ± 0.55
265	271	IVSMLTK	Oxidation M (+15.99)	1.2	404.23	806.46	47.6	32.0	NA	1.95 ± 0.65

Abbreviations: ETS, error tolerant search; NA, not available; SS, standard search
'Start' and 'stop' indicate the amino-acid positions of the peptides. Expected values are annotated when the peptide identifications were derived from the SS, but were not available (NA) when the search result was from the ETS, as it was based on a single-protein database

regardless of PDT. After PDT, activity losses were seen in all three mutants (20–50%) as compared with their respective original activities without PDT (Figure 5a). Similar results were observed for PARP cleavage assays in total cell lysates (Figure 5b). These observations suggest that oxidation of multiple Met residues could contribute to the Photofrin-PDT-mediated oxidative regulation of caspase-3 activity. We then generated a M44L mutant of wild-type procaspase-3 to further evaluate the role of Met-44 in caspase-3 activity regulation. When wild-type procaspase-3 was expressed in *E. coli*, induction triggered its autoprocessing in 1–1.5 h. In contrast, the M44L mutant matured after induction for 2 h (Figure 5c), indicating that substituting Met-44 with Leu slowed the autoprocessing of procaspase-3. Furthermore, we expressed all the procaspase-3 constructs in MCF-7 cells. In addition, we also generated a prodomain deletion mutant ($^\Delta$N) and its M44L mutant ($^\Delta$N-M44L) to test whether this Met-to-Leu mutation had any effect on procaspase-3 processing at Asp-175 (Figure 5d), as it has been well established that during activation, procaspase-3 is first cut at Asp-175 between the large and small subunits, and then at Asp-28 between the prodomain and the large subunit.[25] MCF-7 cells transiently transfected with these expression plasmids were challenged by UV irradiation to trigger caspase-3 activation. All procaspase-3 variants were ectopically expressed in MCF-7 cells at levels similar to that of the wild-type (Figure 5e, upper panel). They could respond to UV irradiation, as evidenced by the detection of active caspase-3 fragments (Figure 5e, middle panel) and increased caspase-3 activity (Figure 5f). The $^\Delta$N mutant was activated more strongly (~2-fold) by UV stress than the wild-type (Figure 5f), which is consistent with a previous report that the prodomain of procaspase-3 may have autoinhibitory

effects.[26] The M44L mutant and the corresponding prodomain deletion mutant ($^\Delta$N-M44L), but not M27L and M39L, inhibited casapase-3 activation as compared with the activations of the wild-type and $^\Delta$N mutant, respectively (Figures 5e and f). These results collectively indicate that the Met-44 residue has an important role in regulating Asp-175 cleavage during caspase-3 maturation.

Discussion

PDT-induced cell apoptosis or necrosis may occur through complicated mechanisms,[27] and PDT-induced inflammatory responses to necrotic tumor cells can elicit a tumor-specific immunity that can have a decisive role in attaining long-term tumor control.[28,29] However, no previous study has investigated whether caspase-3 itself is subject to direct regulation by covalent modification in PDT-treated cells. Here, we report that Photofrin-PDT can directly modify procaspase-3, impair its enzyme activity, and decrease its activation by the upstream activator, caspase-8 (Figures 1 and 2). These findings could explain why higher doses of Photofrin-PDT failed to trigger significant caspase-3 activation in the tested cells (Figure 1). Several studies have reported that the death phenotype can be switched from apoptosis to necrosis-like death by inhibition of caspase-3.[30–32] Our present findings appear to provide a new and important mechanism through which the fate of Photofrin-PDT-treated tumor cells may be determined.

Using two different MS-based quantitative approaches and purified recombinant procaspase-3-D$_3$A, we systemically explored the Photofrin-PDT-triggered modifications of procaspase-3. The results from both strategies showed that Met oxidation represented the major modification of procaspase-3-D$_3$A

Table 2 Analysis of the oxidized peptide yields of procaspase-3-D$_3$A treated with different doses of Photofrin-PDT, as assessed by ^{15}N labeling

Start–Stop	Sequence	Modifications	Charge	Ion score	Identity score	% Of peptide yields					[16]O/[18]O[a]
						Photofrin dose (μg/ml)					Photofrin (μg/ml)
						0	7	14	28	56	28
1–11	MENTENSVASK		2	82	51	100.00	93.93	100.00	100.00	98.28	0.79
1–11	MENTENSVASK	Oxidation M (+15.99)	2	57	47	0.00	6.07	0.00	0.00	1.72	1.27
20–38	IIHGSESMASGISLDNSYK		2.3	167	49	89.98	85.79	70.96	72.96	59.19	1.10
20–38	IIHGSESMASGISLDNSYK	Oxidation M (+15.99)	2.3	130	49	10.02	14.21	29.04	27.04	40.81	5.07
39–53	MDYPEMGLCIIINNK		2	94	53	20.09	17.40	0.00	12.41	0.00	1.41
39–53	MDYPEMGLCIIINNK	Carbamidomethyl (+57.02)	2	118	48	78.42	74.51	48.60	25.03	24.94	1.20
39–53	MDYPEMGLCIIINNK	Oxidation M (+15.99)(M44)	2	73	54	0.00	2.09	0.00	6.87	3.61	NA
39–53	MDYPEMGLCIIINNK	Carbamidomethyl (+57.02), oxidation M (+15.99)(M39 or M44)	2	70	48	1.49	5.99	23.73	26.30	25.90	2.34
39–53	MDYPEMGLCIIINNK	Carbamidomethyl (+57.02), 2 oxidation M (+15.99)	2	92	47	0.00	0.00	27.67	29.38	45.55	NA
65–75	SGTDVDAANLR		2	107	46	100.00	100.00	100.00	100.00	100.00	1.03
80–86	NLKYEVR		2	63	49	100.00	100.00	100.00	100.00	100.00	NA
87–101	NKNDLTREEIVELMR		2.3	64	52	94.93	95.07	92.70	92.74	89.33	NA
87–101	NKNDLTREEIVELMR	Oxidation M (+15.99)	3	36[b]	53	5.07	4.93	7.30	7.26	10.67	NA
89–101	NDLTREEIVELMR		2.3	84	52	100.00	100.00	100.00	100.00	100.00	NA
94–101	EEIVELMR		2	80	47	94.63	93.04	91.55	91.02	89.13	NA
94–101	EEIVELMR	Oxidation M (+15.99)	2	74	46	5.37	6.96	8.45	8.98	10.87	2.09
138–144	KITNFFR		2	57	48	99.34	99.28	99.03	99.05	99.30	1.03
138–144	KITNFFR	Oxidation F (+15.99)	2	48[b]	49	0.66	0.72	0.97	0.95	0.70	NA
139–144	ITNFFR		2	41[c]	49	100.00	100.00	100.00	100.00	100.00	0.97
157–164	LFIIQACR		2	69	49	0.31	0.33	0.58	0.64	0.56	NA
157–164	LFIIQACR	Carbamidomethyl (+57.02)	2	70	47	99.69	99.67	99.42	99.36	99.44	1.18
165–186	GTELDCGIETASG VDDDMACHK	Carbamidomethyl (+57.02)	2.3	71	51	0.00	0.00	0.00	0.50	0.00	NA
165–186	GTELDCGIETASGV DDDMACHK	2 Carbamidomethyl (+57.02)	2.3	122	42	92.58	91.52	89.19	88.48	84.63	1.09
165–186	GTELDCGIETASGVDD DMACHK	2 Carbamidomethyl (+57.02), Oxidation M (+15.99)	2.3	103	41	7.42	8.48	10.81	11.02	15.37	1.50
225–238	QYADKLEFMHILTR		2.3	85	49	100.00	100.00	100.00	83.74	68.50	1.24
225–238	QYADKLEFMHILTR	Oxidation M (+15.99)	2.3	70	50	0.00	0.00	0.00	16.26	31.50	2.28
230–238	LEFMHILTR		2.3	77	51	96.68	94.37	94.43	92.87	89.40	0.92
230–238	LEFMHILTR	Oxidation M (+15.99)	2	51[c]	52	3.32	5.63	5.57	7.13	10.60	1.74
243–259	VATEFESFSFDATFHAK		2.3	103	53	100.00	100.00	0.00	100.00	0.00	1.17
260–271	KQIPCIVSMLTK	Carbamidomethyl (+57.02)	2.3	78	50	94.03	93.70	92.44	90.32	85.02	0.86
260–271	KQIPCIVSMLTK	Carbamidomethyl (+57.02), oxidation M (+15.99)	2.3	65	51	5.97	6.30	7.56	9.47	14.86	1.71
260–271	KQIPCIVSMLTK	Trioxidation C (+47.97)	2	51	48	0.00	0.00	0.00	0.21	0.12	NA
261–271	QIPCIVSMLTK	Carbamidomethyl (+57.02)	2	83	51	93.08	100.00	89.44	92.58	73.36	0.93
261–271	QIPCIVSMLTK	Carbamidomethyl (+57.02), oxidation M (+15.99)	2	38[c]	52	6.92	0.00	10.56	7.42	26.64	1.62

[a]Data were taken from Supplementary Table 1
[b]The ion score of the peptide was lower than the identity score, but it was identified in all five samples
[c]The ion score of the peptide was lower than the identity score, but it was observed in the ^{16}O/^{18}O-labeling experiments

peptides (Tables 1 and 2). The oxidations of Met-27, Met-39 and Met-44 were determined to be the three most prominent modifications. Surprisingly, the modification ratio of the active site (Cys-163)-containing peptide did not change following PDT in both experiments, indicating that either the active site was not modified, or the modification was too minor to be detected by MS. Mapping the susceptible Met residues in the 3D structure of procaspase-3 (PDB code: 1I3O, a.a. 32–174 and 176–277)[33] shows that Met-39 and Met-44 cluster together at the surface of each monomer (Figure 6). In contrast, the active site Cys-163 is located at the interface of the two monomers. This analysis supports the notion that amino-acid residues located at the surface of caspase-3 are more susceptible to Photofrin-PDT-mediated oxidation, and may also explain why we didn't detect oxidation of the active site Cys-163 (i.e., Photofrin could not reach it). Although Met-61 and Met-182 were also exposed on the outside of the dimeric structure, their oxidations were not significant (Tables 1 and 2, and Supplementary Table 1 and 2). This observation further suggests that Photofrin-PDT-mediated Met oxidation shows selectivity. Collectively, we identify the N-terminal region of procaspase-3 that is highly susceptible to
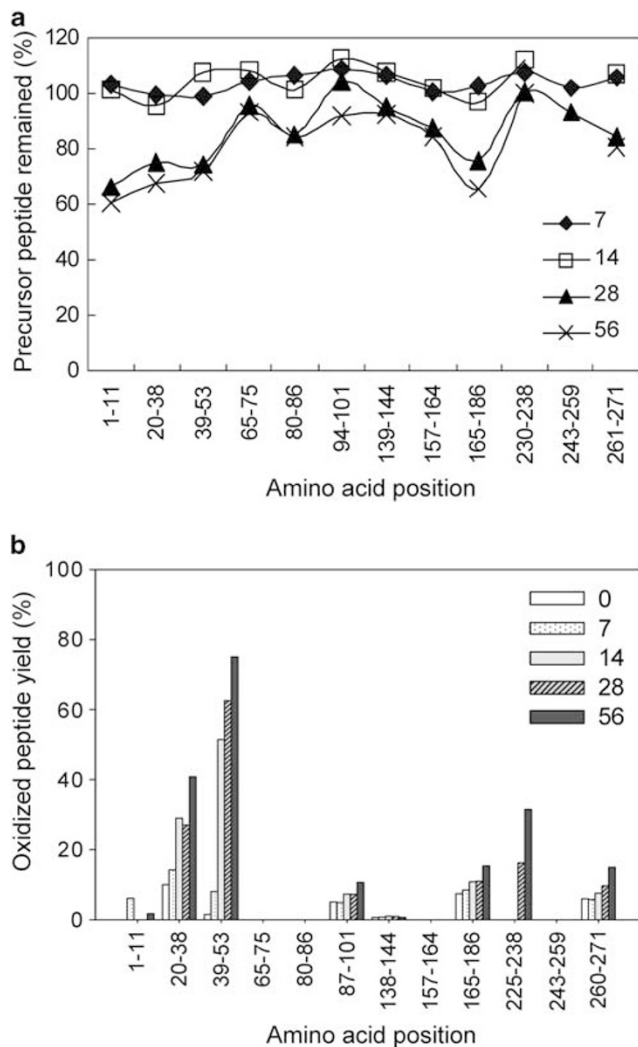
Figure 4 Quantitative analysis of Met oxidation of procaspase-3-D$_3$A at different doses of Photofrin-PDT, as assessed using ^{15}N-labeling. (**a**) Precursor peptides remaining after PDT with different doses of Photofrin. After LC-MS/MS analysis, the amounts of precursor peptides that remained for each detected peptide were calculated from the extracted ion chromatograms derived from the MSQuant results. The PDT *versus* control (^{14}N/^{15}N) ratios of precursor peptides derived from untreated samples (i.e., dosed with 0 μg/ml of Photofrin) were taken as 100%. (**b**) Oxidized peptide yields after PDT with different doses of Photofrin. The oxidized peptide yield for each detected peptide was determined from the extracted ion chromatograms as the proportion of oxidized peptide *versus* that of all possible forms of that particular peptide: oxidized peptide/(oxidized peptide + unmodified precursor peptide + peptides with other modifications). The oxidized peptide yield represented the summation of all kind of oxidations such as single and dual methionine oxidation, cystine trioxidation and so on (see 'Supplementary Materials and Methods'). This calculation assumed that all possible modifications were identified

Photofrin-PDT-mediated oxidative stress by quantitative proteomics approaches.

Numerous studies have reported that Met oxidation can induce functional changes in proteins/peptides.[34,35] Fluorophore-assisted light inactivation treatment also triggers the formation of singlet oxygen, which can cause Met oxidation and inactivation of calmodulin.[36] Modifications of sensitive residues located in a regulatory or catalytic region of the

protein could have a profound effect on its function. Although we have shown that Met oxidation represents the major detectable covalent modification during the Photofrin-PDT-mediated inhibition of caspase-3, the role of Met oxidation in this observed inhibitory process still remains elusive. Our findings that (i) caspase-8-mediated cleavage of procaspase-3 at both Asp-175 and Asp-28 was drastically inhibited by Photofrin-PDT pretreatment (Figure 1), and (ii) the oxidized peptide yield of ^{39}MDYPEMGLCIIINN^{53}K correlated well with the caspase-3 activity loss after Photofrin-PDT (Figures 2 and 4) suggest that Photofrin-PDT-mediated Met-39/44 oxidation of procaspase-3 might interfere with the cleavage/activation process. During the maturation process, procaspase-3 is first cut at Asp-175 and forms the p20/p12 complex,[37] which is catalytically active and can undergo autocleavage at Asp-28 to remove the prodomain and generate the mature p17/p12 caspase-3.[25] Notably, mutation of Met-44 caused the prodomain cleavage without producing activity and inhibition of caspase-3 activation procedure by an apoptotic trigger (UV irradiation) (Figure 5). It is possible that Met-44 has a role in regulating caspase-3 cleavage/activation process, and oxidation of Met-44 may increase the hydrogen bonding to the surrounding amino-acid residues and alter the local structure, thereby affecting the proteolytic maturation of procaspase-3. Further experiments are needed to clarify the detailed mechanism.

PDT has been shown to damage several proteins/enzymes, leading to the loss of their biological activity,[38–40] but little is known about how they are modified and whether they are the direct targets of Photofrin (i.e., Photofrin-binding proteins). We show here for the first time that Photofrin can directly bind to procaspase-3 (Figure 3), and provide evidence that this direct interaction could be the major driving force for the observed modification/inactivation of procaspase-3 during Photofrin-PDT. It is interesting to note that Zawacka-Pankau and colleagues[40] has also reported direct interaction between Fhit and protoporphyrin IX (PpIX), which is the precursor for generating Photofrin. Fhit lost its hydrolase activity following PpIX-PDT *in vitro*, and the H98N mutation inhibits both the Fhit-PpIX interaction and Fhit's tumor-suppressing ability, implying that H98 may be a vulnerable residue for PpIX-PDT and an important residue for Fhit hydrolase activity. These observations collectively suggest that the direct binding of photosensitizers to specific proteins may guide the selectivity of protein modification in PDT-treated cells.

In conclusion, we herein report for the first time that Photofrin-PDT can induce covalent modification of procaspase-3 and impair its activation in a ROS-dependent manner. Photofrin can directly bind to procaspase-3, the ROS formed immediately after laser irradiation can preferentially oxidize procaspase-3 on several Met residues (but not the active site Cys-163), and the Met-44 residue has a critical role in the proteolytic processing of procaspase-3 at Asp-28 and 175. Thus, the present study reveals a novel mechanism through which caspase-3 activity is regulated in tumor cells treated with Photofrin-PDT.

Materials and Methods

Cell culture and Photofrin-PDT. Human epidermoid carcinoma A431 and breast adenocarcinoma MCF-7 cells were cultured at 37°C in DMEM supplemented
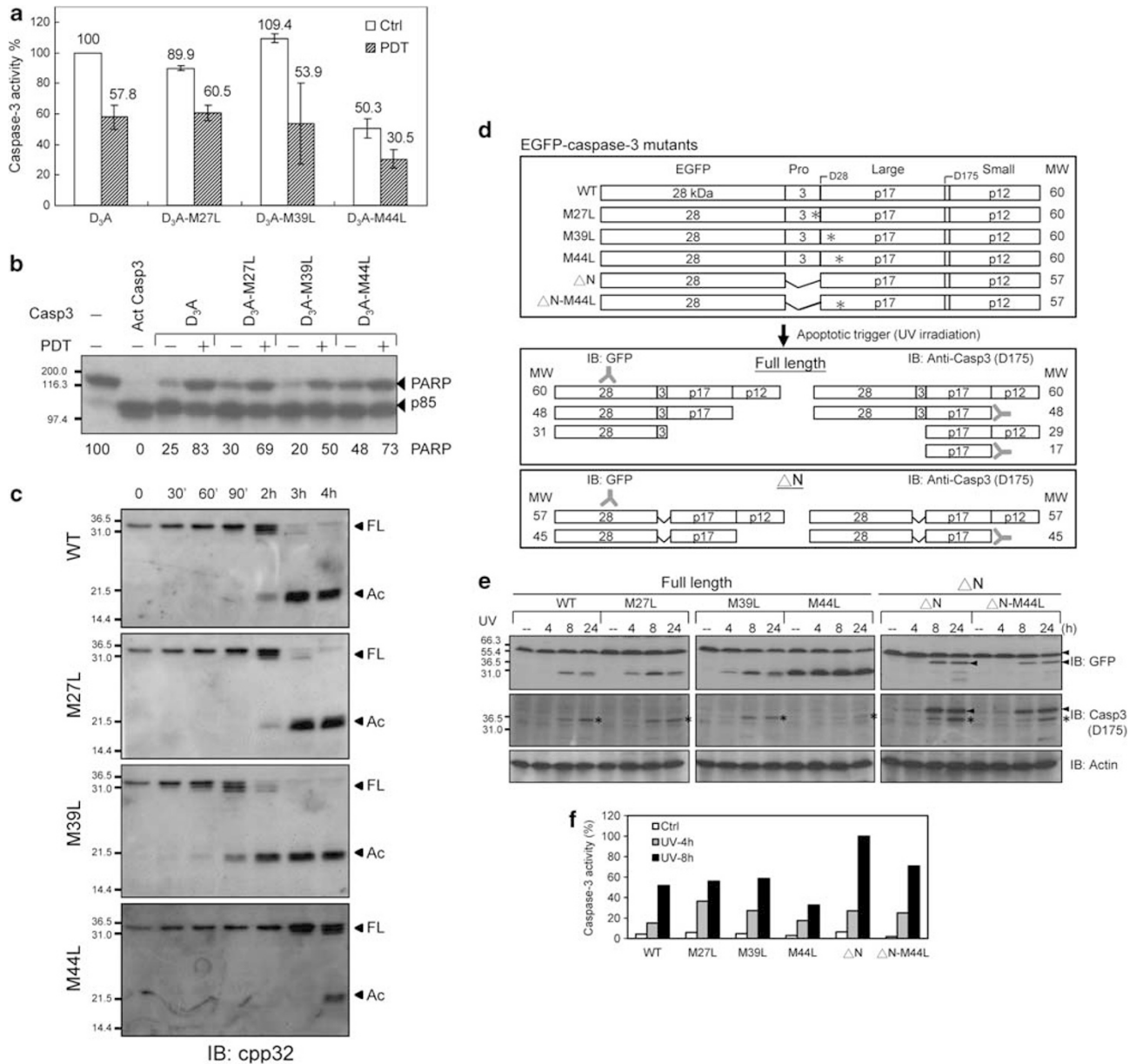
Figure 5 Substitution of Met-44 by Leu attenuates the proteolytic maturation of caspase-3 in *E. coli* and MCF-7 cells. (**a** and **b**) Purified recombinant procaspase-3-D$_3$A and its Met-to-Leu mutants (Met-27, Met-39 and Met-44) were treated with PDT using 28 μg/ml of Photofrin, followed by caspase-3 activity assays using Ac-DEVD-pNA (**a**) or endogenous PARP from A431 cell lysates (**b**). In (**b**), A431 cell lysates (100 μg) were digested with procaspase-3-D$_3$A and its mutants at 37°C for 1 h, resolved by 10% SDS-PAGE, and subjected to immunoblotting with an anti-PARP antibody. 'Act Casp3' denotes the recombinant active form of caspase-3 purified from *E. coli*. (**c**) Wild-type procaspase-3 and its Met-to-Leu mutants were cloned into the pET23a vector, expressed in *E. coli* BL-21(DE3) cells via IPTG induction for different time periods, and analyzed by immunoblotting with an anti-caspase-3 antibody. FL, full-length form of procaspase-3; Ac, activated form of caspase-3. (**d**) Schematic representation of the structures of EGFP-tagged full-length procaspase-3, prodomain-deleted (^ΔN) procaspase-3 and the Met-to-Leu mutants (Met-27, Met-39 and Met-44). The lower panel denotes the predicted MWs of the unprocessed and possible proteolytic forms of caspase-3 found in MCF-7 cells after the application of UV irradiation to trigger apoptosis. (**e** and **f**) Vectors encoding EGFP-tagged full-length procaspase-3, ^ΔN-procaspase-3 or the Met-to-Leu mutants were individually transfected to MCF-7 cells, and the transfected cells were selected with G418 (800 μg/ml) for 2 weeks. The stably selected cells were left untreated or irradiated with UV light (200 J/m^2). Cell lysates were collected at 4, 8 and 24 h and subjected to 15% SDS-PAGE, followed by immunoblot analysis using antibodies against GFP, cleaved caspase-3 (D175) or actin (**e**), or by caspase-3 activity assay using Ac-DEVD-pNA (**f**). The experiments were repeated three times with reproducible results

with 10% heat-inactivated fetal bovine serum, 100 U/ml penicillin, and 100 μg/ml streptomycin. Jurkat T cells were cultured at 37°C in RPMI-1640 supplemented with 10% heat-inactivated fetal bovine serum, 100 U/ml penicillin and 100 μg/ml streptomycin. Cells were incubated in media containing various concentrations of Photofrin (diluted from a 2.5 mg/ml stock solution in 5% dextrose) (Pinnacle Biologics, Inc., Bannockburn, IL, USA) in the dark at 37°C for 3 h, and then irradiated with a

632.8-nm He–Ne laser (Coherent, Santa Clara, CA, USA; fluence rate 15 mW, total energy 10 J/cm^2). The cell culture plates were covered with aluminum foil, and all processes up to the SDS-PAGE step were performed in the dark to avoid unwanted light exposure. After PDT, the cells were washed twice with ice-cold PBS and lysed in lysis buffer (10 mM Tris-HCl, pH 7.4, 1 mM EDTA, 1 mM EGTA, 1% Triton X-100, 1 mM benzamidine, 1 mM phenylmethylsulfonyl fluoride, 50 mM sodium fluoride,
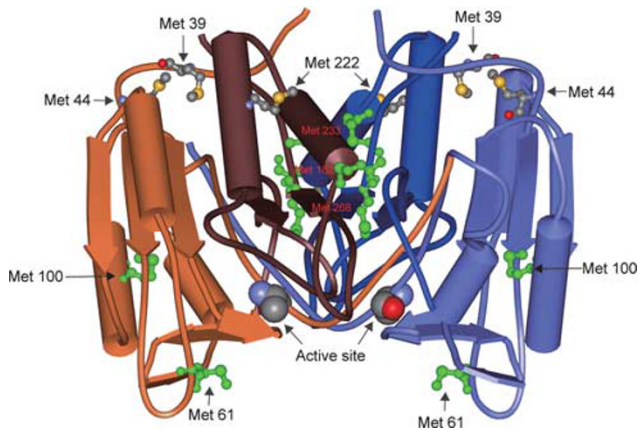
Figure 6 The crystal structure of caspase-3. Positions of the Met residues are denoted in the caspase-3 structure (PDB code: 1I3O[33]). To generate this structure, the active site (Cys-163) of recombinant procaspase-3 was mutated to Ala, and the protein was digested by granzyme and cocrystallized with XIAP. The N-terminal 1–31 residues were not resolved because of granzyme digestion at Asp-28. The orange and blue colors represent the dimeric caspase-3 molecules with their large and small subunits. Met-39, -44 and -222 are shown schematically as ball-and-stick atoms (gray, carbon; yellow, sulfur; and red, oxygen). The active site C163A is shown as a space-filling model. Met residues that did not show significant changes after Photofrin-PDT are indicated in green

20 mM sodium pyrophosphate and 1 mM sodium orthovanadate) on ice for 15 min. The cell lysates were sonicated on ice and collected by centrifugation at 11 000 r.p.m. for 30 min at 4°C, and the protein concentrations were determined with a BCA protein assay reagent (Pierce, Rockford, IL, USA).

Anti-Fas antibody and TRAIL treatments. After PDT treatment, Jurkat T cells (5×10^6/ml) were treated with 500 ng Fas antibody (Clone CH.11, Millipore Upstate, Billerica, MA, USA) or TRAIL (PeproTech, Rocky Hill, NJ, USA) for 6 h. The cell lysates were then collected and analyzed by immunoblotting and caspase-3 activity assay.

Immunoblotting. Immunoblotting was carried out essentially as described.[8] The monoclonal anti-CPP32/caspase-3 antibody was from Transduction Laboratories (Lexington, KY, USA); the anti-PARP, anticleaved caspase-3 (D175), anti-caspase-8 and anti-caspase-9 antibodies were from Cell Signaling Technology (Beverly, MA, USA); the anti-actin antibody was from Millipore (Billerica, MA, USA); and the anti-His antibody was from Santa Cruz Biotechnology (Santa Cruz, CA, USA). These antibodies were used to probe proteins transferred from SDS gels onto PVDF membranes, and the resulting signals were quantified by a densitometer (GE Healthcare Bio-Science, Uppsala, Sweden).

Plasmid construction. The full-length human caspase-3 gene was amplified by PCR using cDNAs derived from human epidermoid carcinoma A431 cells as templates, and primers containing *Nde*I/*Xho*I sites (*Nde*I, 5'-GGAATTCCATATGGAGAACACTGAAAACTCAG-3'; *Xho*I, 5'-CCGCTCGAGG TGATAAAAATAGAGTTCTTTTGTG-3'). Purified PCR products were digested by *Nde*I and *Xho*I and cloned into the respective sites of a pET23a vector (Merck KGaA, Darmstadt, Germany) to generate the pET23a-caspase-3 expression plasmid. To produce the pET23a-caspase-3-D$_3$A mutant, in which the cleavage sites at D9, -28 and -175 were substituted to alanines, we used the following forward and reverse primers: D9A-f, 5'-CATATGGAGAACACTGAAAACTCAGT GCTTCAAAATCC-3'; D9A-r, 5'-GGATATTCCAGAGGCCATTGATTCGCT-3'; D28 A-f, 5'-GAATCAATGGCCTCTGGAATA-3'; D28A-r, 5'-AACACCACTGGCTGTCTC AAT-3'; D175A-f, 5'-GGCATTGAGACAGCCAGTGGTGTGAT-3'; D175A-r, 5'-TGTT AGCAGCCGGATCTCAGTGG-3'. We first amplified three fragments by paired primers: M1-D28 (fragment 1), D28-D175 (fragment 2) and D175-H285 (fragment 3). After PCR product purification, we used fragment 1 and 2 as templates, D9A-f and D28A-f as primers to generate fragment M1-D175 (fragment 1 + 2). At last, we used fragment 1 + 2 and fragment 3 as templates, D9A-f and D175A-r as primers to

generate full-length caspase-3 contained D$_3$A mutations. After PCR amplification, we used digestion and ligation to generate the pET23a-caspase-3-D$_3$A mutant. To construct the Met-to-Leu mutants of caspase-3 and caspase-3-D$_3$A, Met-27, -39 and -44 were substituted to Leu using a QuikChange site-directed mutagenesis kit (Stratagene, La Jolla, CA, USA) and specific primers (M27L, 5'-GGAATATCCCTGG ACAACAGTTATAAACTGGATTATCCTGAG-3'; M39L, 5'-ACAACAGTTATAAAAT GGATTATCCTGAGCTGGGTTTATGTATAATAATTAATAATAAG-3'; and M44L, 5'-CC AGTCGCTTTGTGCCCTGCTGAAACAGTATGC-3'). The resulting constructs were also subcloned into the pET23a-caspase-3, pET23a-caspase-3-D$_3$A and pEGFP-C3 vectors (Clontech Laboratories Inc., Mountain View, CA, USA). To generate the prodomain deletion mutant, caspase-3-$^\Delta$N, we amplified pEGFP-C3-procaspase-3 with specific primers ($^\Delta$N-*Eco*RI-f, 5'-GAATTCCGTCTGGAATATCC CTGGACAAC-3'; *Kpn*I-r, 5'-CGCCGGTACCTTAGTGATAAAAATAGAGTTCTTT TG-3'), digested the amplified fragments and ligated them into the above-described vectors. Caspase-3-$^\Delta$N-M44L was also generated using a site-directed mutagenesis kit and the M44L primer. The DNA sequences of all constructs were confirmed by autosequencing.

Purification of recombinant caspase-3. *E. coli* BL21(DE3)-pLysS cells were transformed with pET23a-caspase-3, pET23a-caspase-3-D$_3$A or the various methionine-to-leucine mutants. The transformed *E. coli* were grown and subjected to IPTG induction for 3 h, and the cultures were harvested and purified on His-Trap-FF columns (GE Healthcare Bio-Science, Piscataway, NJ, USA). The fractions containing recombinant proteins were concentrated and desalted with Amicon Centricon filters (5-kDa cutoff; Millipore), and the purified proteins were resuspended in distilled water or the caspase-3 activity assay buffer (see below).

Caspase-3 activity assay. Caspase-3 activity was determined using the Ac-DEVD-pNA colorimetric substrate (Merck KGaA). Briefly, cell lysates (100 μg) or recombinant caspase-3 (10 μg) were incubated in 0.1 ml caspase assay buffer (50 mM HEPES, pH 7.4, 0.1% CHAPS, 10 mM DTT, 0.1 mM EDTA, 100 mM NaCl and 10% glycerol) containing 0.2 mM Ac-DEVD-pNA at 37°C for 30–120 min, and the relative caspase-3 activities were determined by spectrophotometry at 405 nm. In some experiments, the relative activities of recombinant caspase-3 proteins were measured by their abilities to cleave the PARP protein to produce a 85 kDa fragment in cell lysates (100 μg), as detected by immunoblotting.

Annexin V and propidium iodide staining and flow cytometry. A431 and Jurkat T cells were treated with different doses of Photofrin-PDT. After 6 h incubation, cells were stained by FITC Annexin V Apoptosis Detection Kit (BD Biosciences, San Jose, CA, USA) and analyzed by FACSCalibur (BD Biosciences).

Gel filtration analysis. Recombinant procaspase-3-D$_3$A alone (1 mg), Photofrin alone (18.13 μg) or procaspase-3-D$_3$A (1 mg) plus Photofrin (18.13 μg) (molar ratio 1 : 1) were applied to Superose 12 HR 10/30 columns (GE Healthcare Bio-Science) pre-equilibrated with buffer A (0.05 M phosphate buffer with 0.15 M NaCl, pH 7.0). Fractions (1 ml) were collected and assessed by optical density measurement (280 nm) for procaspase-3-D$_3$A proteins and by fluorescence measurement (excitation 400 nm and emission 630 nm) for Photofrin. Fractions were also directly spotted onto PVDF membranes, and procaspase-3-D$_3$A and Photofrin signals were detected by immunoblotting and fluorescence scanning (Typhoon 9400; GE Healthcare), respectively.

Plasmid transfection and UV treatment. MCF-7 cells were separately transfected with various caspase-3 mutant plasmids using Lipofectamine 2000 (Invitrogen, Carlsbad, CA, USA) according to the provided protocol. After 24 h expression, transfected cells were irradiated by UV light (200 J/m^2) and the cell lysates were harvested after 4 or 8 h incubation for immunoblotting and caspase-3 activity assay.

Mass spectrometry data analysis. The intact protein measurement, ^{16}O/^{18}O labeling, ^{14}N/^{15}N labeling and mass spectrometry-related sample preparation and data analysis are detailed in the Supplementary Materials and Methods.

Conflict of Interest

The authors declare no conflict of interest.

1. Oleinick NL, Morris RL, Belichenko I. The role of apoptosis in response to photodynamic therapy: what, where, why, and how. *Photochem Photobiol Sci* 2002; **1**: 1–21.
2. Kessel D, Vicente MG, Reiners JJ Jr. Initiation of apoptosis and autophagy by photodynamic therapy. *Autophagy* 2006; **2**: 289–290.
3. Marchal S, Fadloun A, Maugain E, D'Hallewin MA, Guillemin F, Bezdetnaya L. Necrotic and apoptotic features of cell death in response to Foscan photosensitization of HT29 monolayer and multicell spheroids. *Biochem Pharmacol* 2005; **69**: 1167–1176.
4. Agarwal ML, Clay ME, Harvey EJ, Evans HH, Antunez AR, Oleinick NL. Photodynamic therapy induces rapid cell death by apoptosis in L5178Y mouse lymphoma cells. *Cancer Res* 1991; **51**: 5993–5996.
5. Dellinger M. Apoptosis or necrosis following Photofrin photosensitization: influence of the incubation protocol. *Photochem Photobiol* 1996; **64**: 182–187.
6. Peng Q, Moan J, Nesland JM. Correlation of subcellular and intratumoral photosensitizer localization with ultrastructural features after photodynamic therapy. *Ultrastruct Pathol* 1996; **20**: 109–129.
7. Hsieh YJ, Wu CC, Chang CJ, Yu JS. Subcellular localization of Photofrin determines the death phenotype of human epidermoid carcinoma A431 cells triggered by photodynamic therapy: when plasma membranes are the main targets. *J Cell Physiol* 2003; **194**: 363–375.
8. Hsieh YJ, Yu JS, Lyu PC. Characterization of photodynamic therapy responses elicited in A431 cells containing intracellular organelle-localized photofrin. *J Cell Biochem* 2010; **111**: 821–833.
9. Wyld L, Reed MW, Brown NJ. Differential cell death response to photodynamic therapy is dependent on dose and cell type. *Br J Cancer* 2001; **84**: 1384–1386.
10. Boatright KM, Salvesen GS. Mechanisms of caspase activation. *Curr Opin Cell Biol* 2003; **15**: 725–731.
11. Mannick JB, Hausladen A, Liu L, Hess DT, Zeng M, Miao QX et al. Fas-induced caspase denitrosylation. *Science* 1999; **284**: 651–654.
12. Huang Z, Pinto JT, Deng H, Richie JP Jr. Inhibition of caspase-3 activity and activation by protein glutathionylation. *Biochem Pharmacol* 2008; **75**: 2234–2244.
13. Alvarado-Kristensson M, Melander F, Leanderson K, Ronnstrand L, Wernstedt C, Andersson T. p38-MAPK signals survival by phosphorylation of caspase-8 and caspase-3 in human neutrophils. *J Exp Med* 2004; **199**: 449–458.
14. Mikes J, Kleban J, Sackova V, Horvath V, Jamborova E, Vaculova A et al. Necrosis predominates in the cell death of human colon adenocarcinoma HT-29 cells treated under variable conditions of photodynamic therapy with hypericin. *Photochem Photobiol Sci* 2007; **6**: 758–766.
15. Furre IE, Moller MT, Shahzidi S, Nesland JM, Peng Q. Involvement of both caspase-dependent and -independent pathways in apoptotic induction by hexaminolevulinate-mediated photodynamic therapy in human lymphoma cells. *Apoptosis* 2006; **11**: 2031–2042.
16. Chen Y, Zheng W, Li Y, Zhong J, Ji J, Shen P. Apoptosis induced by methylene-blue-mediated photodynamic therapy in melanomas and the involvement of mitochondrial dysfunction revealed by proteomics. *Cancer Sci* 2008; **99**: 2019–2027.
17. Bertrand R, Solary E, O'Connor P, Kohn KW, Pommier Y. Induction of a common pathway of apoptosis by staurosporine. *Exp Cell Res* 1994; **211**: 314–321.
18. Janicke RU, Sprengart ML, Wati MR, Porter AG. Caspase-3 is required for DNA fragmentation and morphological changes associated with apoptosis. *J Biol Chem* 1998; **273**: 9357–9360.
19. Denault JB, Salvesen GS. Expression, purification, and characterization of caspases. *Curr Protoc Protein Sci* 2003; **Chapter 21**: Unit 21 13.
20. Bose K, Pop C, Feeney B, Clark AC. An uncleavable procaspase-3 mutant has a lower catalytic efficiency but an active site similar to that of mature caspase-3. *Biochemistry* 2003; **42**: 12298–12310.
21. Moan J, Berg K. The photodegradation of porphyrins in cells can be used to estimate the lifetime of singlet oxygen. *Photochem Photobiol* 1991; **53**: 549–553.
22. Kessel D, Castelli M, Reiners JJ. Ruthenium red-mediated suppression of Bcl-2 loss and $Ca(2+)$ release initiated by photodamage to the endoplasmic reticulum: scavenging of reactive oxygen species. *Cell Death Differ* 2005; **12**: 502–511.
23. Magi B, Ettorre A, Liberatori S, Bini L, Andreassi M, Frosali S et al. Selectivity of protein carbonylation in the apoptotic response to oxidative stress associated with photodynamic therapy: a cell biochemical and proteomic investigation. *Cell Death Differ* 2004; **11**: 842–852.
24. Qian WJ, Monroe ME, Liu T, Jacobs JM, Anderson GA, Shen Y et al. Quantitative proteome analysis of human plasma following *in vivo* lipopolysaccharide administration using $^{16}O/^{18}O$ labeling and the accurate mass and time tag approach. *Mol Cell Proteomics* 2005; **4**: 700–709.
25. Han Z, Hendrickson EA, Bremner TA, Wyche JH. A sequential two-step mechanism for the production of the mature p17:p12 form of caspase-3 *in vitro*. *J Biol Chem* 1997; **272**: 13432–13436.
26. Meergans T, Hildebrandt AK, Horak D, Haenisch C, Wendel A. The short prodomain influences caspase-3 activation in HeLa cells. *Biochem J* 2000; **349**(Pt 1): 135–140.
27. Buytaert E, Dewaele M, Agostinis P. Molecular effectors of multiple cell death pathways initiated by photodynamic therapy. *Biochim Biophys Acta* 2007; **1776**: 86–107.
28. Castano AP, Mroz P, Hamblin MR. Photodynamic therapy and anti-tumour immunity. *Nat Rev Cancer* 2006; **6**: 535–545.
29. Garg AD, Nowis D, Golab J, Agostinis P. Photodynamic therapy: illuminating the road from cell death towards anti-tumour immunity. *Apoptosis* 2010; **15**: 1050–1071.
30. Xiang J, Chao DT, Korsmeyer SJ. BAX-induced cell death may not require interleukin 1 beta-converting enzyme-like proteases. *Proc Natl Acad Sci USA* 1996; **93**: 14559–14563.
31. Hirsch T, Marchetti P, Susin SA, Dallaporta B, Zamzami N, Marzo I et al. The apoptosis-necrosis paradox. Apoptogenic proteases activated after mitochondrial permeability transition determine the mode of cell death. *Oncogene* 1997; **15**: 1573–1581.
32. Vercammen D, Beyaert R, Denecker G, Goossens V, Van Loo G, Declercq W et al. Inhibition of caspases increases the sensitivity of L929 cells to necrosis mediated by tumor necrosis factor. *J Exp Med* 1998; **187**: 1477–1485.
33. Riedl SJ, Renatus M, Schwarzenbacher R, Zhou Q, Sun C, Fesik SW et al. Structural basis for the inhibition of caspase-3 by XIAP. *Cell* 2001; **104**: 791–800.
34. Yamniuk AP, Ishida H, Lippert D, Vogel HJ. Thermodynamic effects of noncoded and coded methionine substitutions in calmodulin. *Biophys J* 2009; **96**: 1495–1507.
35. Schoneich C. Methionine oxidation by reactive oxygen species: reaction mechanisms and relevance to Alzheimer's disease. *Biochim Biophys Acta* 2005; **1703**: 111–119.
36. Yan P, Xiong Y, Chen B, Negash S, Squier TC, Mayer MU. Fluorophore-assisted light inactivation of calmodulin involves singlet-oxygen mediated cross-linking and methionine oxidation. *Biochemistry* 2006; **45**: 4736–4748.
37. Pop C, Chen YR, Smith B, Bose K, Bobay B, Tripathy A et al. Removal of the pro-domain does not affect the conformation of the procaspase-3 dimer. *Biochemistry* 2001; **40**: 14224–14235.
38. Kim SY, Tak JK, Park JW. Inactivation of NADP(+)-dependent isocitrate dehydrogenase by singlet oxygen derived from photoactivated rose bengal. *Biochimie* 2004; **86**: 501–507.
39. Suto D, Sato K, Ohba Y, Yoshimura T, Fujii J. Suppression of the pro-apoptotic function of cytochrome c by singlet oxygen via a haem redox state-independent mechanism. *Biochem J* 2005; **392**(Pt 2): 399–406.
40. Ferens B, Kawiak A, Banecki B, Bielawski KP, Zawacka-Pankau J. Aberration of the enzymatic activity of Fhit tumor suppressor protein enhances cancer cell death upon photodynamic therapy similarly to that driven by wild-type Fhit. *Cancer Lett* 2009; **280**: 101–109.

Supplementary Information accompanies the paper on Cell Death and Disease website (http://www.nature.com/cddis)